# Image-Guided Locomotion of a Pneumatic-Driven Peristaltic Soft Robot

Matheus S. Xavier, Andrew J. Fleming and Yuen K. Yong
*Precision Mechatronics Lab, School of Electrical Engineering and Computing*
*The University of Newcastle*
*Callaghan, NSW 2308, Australia*
{*matheus.xavier, andrew.fleming, yuenkuan.yong*}*@newcastle.edu.au*

***Abstract*— In this work, a pneumatic-driven peristaltic soft robot with pressure feedback control and image-guided tracking is developed. Locomotion is achieved in tube-like environments by mimicking the peristaltic motion of earthworms. The soft actuators are made of silicone rubber with 3D molding and fiber reinforcements. Pressure control is performed using custom-made syringe pumps and on/off controllers in Arduino. Real-time visual tracking is accomplished in OpenCV with a color-based approach. The soft robot has a stroke of 30-35 mm for each cycle of actuation. This pneumatic soft robot shows great potential for application in minimally invasive surgery due to its compliance and biocompatibility.**

***Index Terms*— Bio-inspired robotics, soft robotics, syringe pump, pressure control, image-based tracking.**

## I. Introduction

Differently from conventional manipulators [1], continuum robots have infinite degrees of freedom with elastic structures and no rigid links [2], [3]. Soft robots are continuum robots composed of highly deformable and compliant materials. They display high dexterity and safety but with low accuracy and difficult motion control and sensing [4], [5]. When driven with pressure, soft robots can output high force densities, i.e. high power-to-weight ratio, and are relatively inexpensive [6].

The majority of soft robots are composed of soft fluidic actuators. Soft actuators are commonly manufactured with the aid of additive manufacturing. In most cases, molds are 3D-printed into which silicones are cast and consolidated. The use of 3D printing allows the design of complex features and high precision molds with a lower number of manufacturing steps [7], [8]. Using specifically engineered anisotropic flexible structures, soft actuators can be made to display four different types of motion: extension, contraction, bending and twisting [9]. Fiber reinforcements can be added along the length of the actuators to achieve these different motions. Double helical wrapping, for example, will restrict the ballooning effect in soft actuators and increase extension strokes [10].

Soft robotics are utilized in a broad range of biomedical applications [11]. Due to their compliance and biocompatibility, soft robots can be safely used with surrounding organs and tissues. Fluid-driven soft robots have been applied to endoscopes and steerable catheters, given that they do not rely on high temperatures, electric or magnectic fields. Moreover, they show high bending capability and are unlikely to perforate tissue [12], [13].

The locomotion of soft robots has been reviewed in [14]. One type of locomotion relevant for minimally invasive procedures is peristaltic crawling, whereby longitudinal muscles are contracted in the anchoring segments, while circumferential muscles are contracted in the advancing segments [15]. Peristaltic robots actuated by shape memory alloys [16], magnetic fluids [17] and electric motors [18] have been proposed. Recently, fluid-driven soft peristaltic robots composed of three artificial muscles were discussed in [19], [20]. They consist of a back radial actuator, a central axial actuator and a frontal radial actuator. The posterior and anterior actuators are used to anchor the robot, while the central actuator is used to extend and contract the robot. This mechanism can be used to develop catheters and endoscopes to navigate inside the human digestive and circulatory systems with little human intervention [19].

Fluid-driven soft robots usually employ a pump and system of valves to control the flow rate or pressure inside the actuators [21]–[23]. An alternative method involves the use of syringe pumps. Commercially available syringe pumps, however, are expensive and typically designed for small volumes [24]. Considering these issues, low-cost volumetric control systems using syringe pumps have been investigated in the literature [25]. In order to convert the rotational motion of the motors into linear motion of the syringe plunger, syringe pumps can rely on a rack and pinion [26], [27] or lead-screw mechanisms [24], [28]–[30]. In the latter, the motor rotates a threaded rod that drives a nut attached to a 3D printed syringe plunger adapter.

Visual sensing can be used to determine the position and orientation of the soft robot for modelling or feedback control [31]–[33]. Model-less feedback control for continuum robots has been described in [34]–[36]. This method avoids the accurate model formulation and calibration between camera and robot required in model-based approaches [34], which is particularly relevant considering the complicated kinematic and dynamic models required for soft robots and interaction

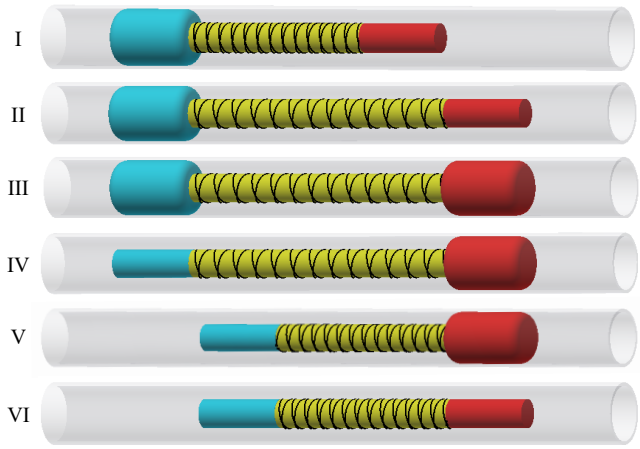


Fig. 1: Order of actuation for peristaltic motion: (I) lock bottom actuator, (II) extend fiber-reinforced actuator, (III) lock top actuator, (IV) release bottom actuator, (V) release fiber-reinforced actuator, and (VI) release top actuator.

with the external environment. While shape-based [34] and colour-based tracking [35], [37] have been studied for concentric tube robots, few works describe the application of visual servoing to soft robots [36].

### A. Contributions of this work

This paper presents a soft peristaltic robot constructed using a fiber-reinforced extending actuator, and two radial actuators for locking. The soft robot is pneumatically driven using three custom-made syringe pumps. Soft peristaltic robots driven pneumatically have been proposed in [19], [20]. This work extends the techniques presented in [19], [20] by combining pressure feedback with real-time, image-guided tracking. The soft robot has a stroke of 30-35 mm for each cycle of actuation, despite variations in the pressure readings and brightness during crawling.

## II. Design and Fabrication

### A. Soft robot

The soft peristaltic robot consists of two locking actuators and an extending actuator as shown in Fig. 1. The order of actuation is shown in the figure. The locking actuator has no fiber wrapping. When pressurized, it expands radially resulting in a balloon shape for locking to the inside wall of a tube. On the other hand, the extending actuator is wrapped in fiber to constrain radial expansion and maximize longitudinal extension.

The soft actuator has a length of 90 mm, diameter of 16.7 mm and thickness of 2 mm [38]. The fabrication process is shown in Fig. 2. Molds are designed in Autodesk Inventor and 3D printed using a Form 2 (Formlabs). Silicone rubber (DragonSkin 10) is mixed at a 1:1 ratio and degassed. The left and right molds are clamped together and the mixture

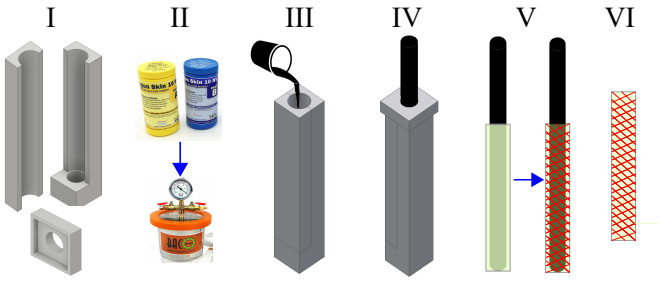


Fig. 2: Fabrication of fiber-reinforced soft actuator: (I) design and 3D print molds, (II) mix and degass silicone rubber, (III) clamp molds and pour rubber, (IV) insert rod and cap molds, (V) after 5 hours, remove molds, add and secure fiber wrapping, and (VI) remove soft actuator and cap both ends.

is poured into the mold. A cylindrical rod is inserted into the mold and held in place with a cap at the top of the mold, which is then left to cure for 5 hours. For the locking actuators, the main body is removed from the mold and capped at both ends with silicone rubber. For the extending actuators, a double wrapping of Kevlar fiber is added and secured in position with a thin layer of silicone rubber. The actuator is then removed from the rod and capped at both ends with a thick layer of silicone rubber. Finally, extension sets of 75 cm (Terumo 5SF*ET0727L22) are inserted into the actuators and held in place by silicone glue.

### B. Syringe pump

The three syringe pumps are fabricated to operate with 50 mL syringes. Components of the syringe pump are shown in Fig. 3. The motor adapter, syringe plunger adapter and syringe holder are designed in Inventor and 3D printed using the Form 2 printer. The stepper motor is secured to the motor adapter, which is then connected to the syringe holder using four outer M6 threaded rods. The threaded rods are fixed using washers and nuts on both sides of the motor adapter and syringe holder. A nut is inserted into the plunger adapter as shown in Fig. 3. An 8 mm lead screw is connected to the motor using a coupler at one end, and through the nut of the plunger adapter to the syringe holder at the other end. The motion of the plunger adapter is guided by two linear shafts and bearings. The stepper motor drives the nut, which, in turn, moves the plunger adapter linearly. The hole in the syringe holder is made 0.5 mm smaller than the syringe diameter in order to secure the syringe in place while the plunger is moved along the pump. A full bill of materials is given in Table I in the appendix.

## III. Experimental Setup

The experimental setup of the peristaltic robot with pressure control and image-based tracking as shown in Fig. 4 is presented in this section.

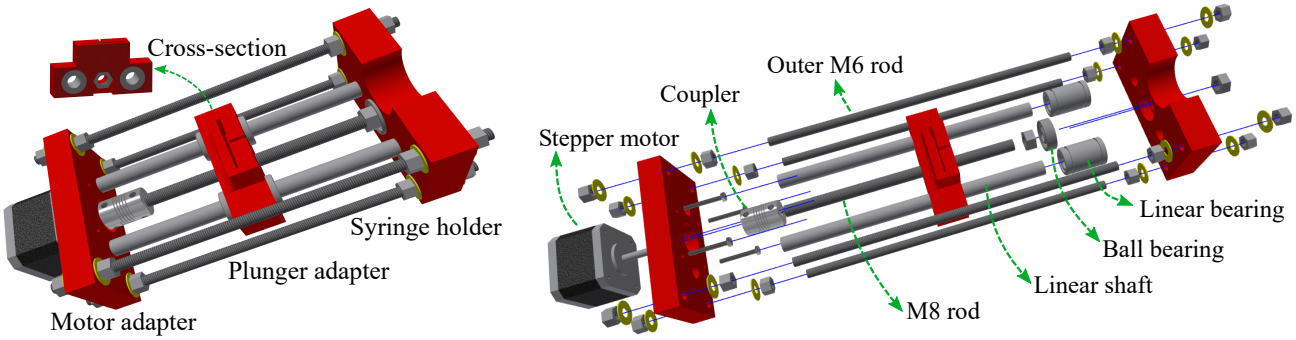


(a) 3D model of syringe pump.

(b) Exploded view.

Fig. 3: Syringe pump. The 3D printed components are shown in red. A cross-section of the syringe plunger adapter in (a) displays the nut through which the 8 mm threaded rod is inserted in the lead-screw mechanism. The exploded view in (b) shows the order of assembly of the components.

### A. *Color-based tracking with OpenCV*

In this work, color-based object tracking [39], [40] via Python/OpenCV is employed to track blue markers attached to the tip of the soft robot and a desired position in the tube. This approach is chosen since color is relatively constant under viewpoint changes and easy to be acquired [41], resulting in high tracking accuracy. Image acquisition is performed using a webcam (Logitech C920) mounted on top of a box frame. The tracking algorithm is described in Fig. 5. Firstly, the video is captured, blurred and converted to HSV model. Hue, saturation and value parameters for the markers are obtained using a trackbar. After that, a mask is created from the values in the range selected with the trackbar and applied to the original image (Fig. 6a). Canny edge detection is used to find the contours in the thresholded image. These contours are sorted and used to determine the centers of the markers via image moments (Fig. 6b). Finally, the distance detween the two markers is determined and filtered using a 4-point moving average (MA) filter to reduce noise. If this distance is higher than 15 pixels (approximately 1.4 cm), a flag '0' is sent to Arduino. Otherwise, a flag '1' is sent to Arduino, which corresponds to the target position being reached.

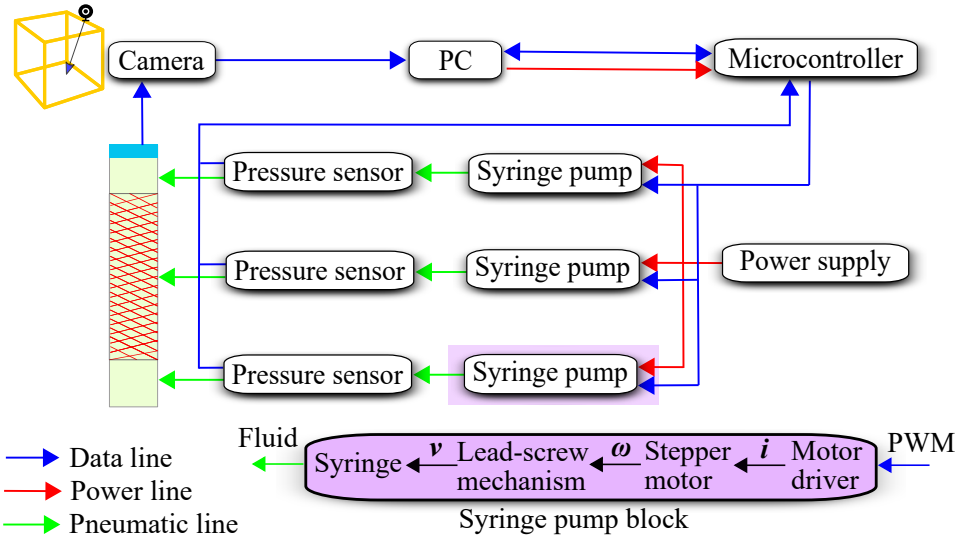


Fig. 4: System architecture for automatic peristaltic motion. Pressure sensors are added between the outputs of the syringe pumps and the soft actuators, while a camera mounted on top of a box frame tracks the tip of the soft robot. The syringe pump block is shown as an inset in the diagram. The motor driver receives the digital square wave signal (PWM) from Arduino and applies current ($i$) to the electromagnetic coils surrounding the shaft of the motor. The angular velocity of the motor ($\omega$) is then converted to linear velocity of the syringe plunger ($v$) via the lead-screw mechanism.

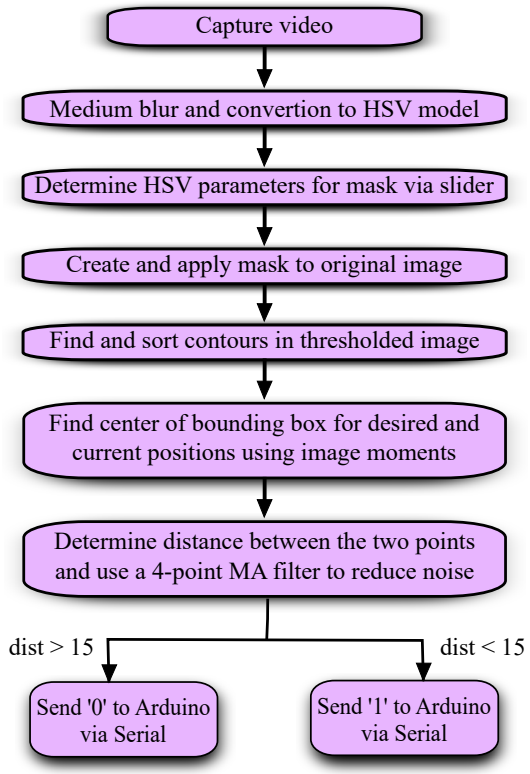


Fig. 5: Diagram of object tracking in OpenCV. The first steps are used to acquire the position of the markers in the soft robot and target location, while the last step is used to send a flag to Arduino.

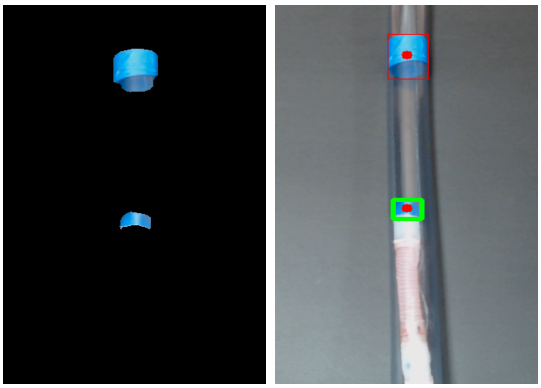

(a) Mask (b) Original video

Fig. 6: Color-based tracking in OpenCV. In (a) the mask is obtained by color thresholding, followed by identification of bounding boxes and respective centers in (b).

### *B. Pressure control with Arduino*

The three stepper motors are connected to a motor driver each. The motor drivers are then connected to a power supply set at 25 V. After setting the current limit in each driver

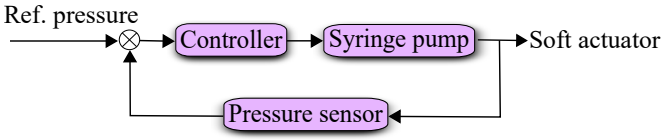


Fig. 7: Block diagram of pressure control loop implemented in each syringe pump.

and connecting the stepper motor wires, an Arduino MEGA 2560 was used to control the frequency of the pulses sent to the motor driver and, consequently, the motor speed. Using 5 mm tubes and extension sets, the outlets of the syringes were connected to the soft actuators. Analog pressure sensors were added to the fluid path via tee connectors in order to perform feedback control. The required pressures for each component of the soft robot are determined and Algorithm 1 is implemented in Arduino to perform the peristaltic motion. Pressure control is achieved using an on/off controller based on the pressure readings from the sensor and the required pressure (Fig. 7).

## IV. Results and Discussion

The soft actuators were characterized by manually actuating a syringe, measuring the pressure and recording the motion with a video camera (60 fps). The images were post-processed using Kinovea to measure the extensions. The radial actuators showed a diameter expansion of 18-30 mm at pressures of 40-60 kPa, while the fiber-reinforced actuator showed an axial extension of 35-45 mm at 80-100 kPa. Consequently, the required pressures for peristaltic climbing were determined to be approximately 50 kPa for the locking components and 100 kPa for the extending component.

Using the color slider programmed in Python, the HSV parameters for the mask were selected as low hue of 44, low saturation of 78 and low value of 160, all remaining high values were left at 255. Once the objects were identified, the power supply was turned on allowing the peristaltic motion to occur. The soft robot had a stroke of 30-35 mm for each cycle of actuation, which lasted 45 s. This is in agreement with results found in the literature: 35 mm after a motion period in [42] and 0.96 mm/s in [16]. It is important to note that, although the stroke could be improved by applying larger pressures to the axial extending actuator, this resulted in fluid leakage at the tube connection with the actuator.

The soft robot operates effectively despite variations in the pressure readings from the sensor and brightness as the robot climbs the pipe, which results from the single camera location. Furthermore, considering the high range of expansion of the back and frontal radial actuators (expansion of approximately three times the initial 16.7 mm diameter), the soft robot can be used to inspect tube-like environments with significant diameter variations.

**Algorithm 1:** Pressure control with image-based tracking

```
Define reference pressures for each actuator;
Set up pins and variables for motor drivers and
  pressure sensors;
while tracking not complete do
    Import OpenCV flag from serial;
    if flag = 0 then
        Measure pressure error (error 1) for bottom
          locking actuator;
        while error1 > 0.1 do
            Drive first linear actuator forward;
        end
        Measure pressure error (error 2) for extending
          actuator;
        while error2 > 0.1 do
            Drive second linear actuator forward;
        end
        Measure pressure error (error 3) for top
          locking actuator;
        while error3 > 0.1 do
            Drive third linear actuator forward;
        end
        Drive first linear actuator backwards;
        Drive second linear actuator backwards;
        Drive third linear actuator backwards;
    end
    if flag = 1 then
        Wait 2 seconds;
    end
end
```

## V. Conclusions

A pneumatic-driven peristaltic soft robot was developed and controlled using pressure feedback control and image-guided tracking. The robot is capable of crawling tube-like environments by mimicking the motion of earthworms. This work further demonstrates the promise of using low-cost, easy-to-use, reprogrammable syringe pumps as the actuation mechanism for fluid-driven soft robots. Segmentation by color thresholding was used to detect a marker on the soft robot and on the desired location at the tube. Peristaltic climbing is performed until the distance between these two points is less than 1.4 cm. Readily available, open-source hardware and software were used in the fabrication of the syringe pump and implementation of visual tracking.

Soft robots are highly compliant and can be actuated using physiological saline as the driving fluid, enabling safe application to biomedical devices. The device described in this work, in particular, can be applied to peristaltic endoscopes and steerable catheters. Future work includes the development of a mathematical model relating the torque and angular velocity of the motors to the flow and pressure of the actuators and driving lines, which is expected to enable prediction and optimization of performance. Fabrication methods for miniaturization are also under investigation.


## Acknowledgment

The authors would like to thank Phillip Dombkins for the support with 3D printing and assembly of the syringe pumps.


## Appendix

TABLE I: Bill of materials.

| Component | Quantity |
|---|---|
| Stepper Motor (SM-42BYG011-25) | 3 |
| Motor Driver (DRV8825) | 3 |
| Motor Coupler (ADA1176) | 3 |
| Arduino Mega 2560 | 1 |
| Breadboard | 1 |
| 50 mL Plastic Syringe | 3 |
| Pressure Sensor (SEN0257) | 3 |
| Tee Connector (6 mm OD, 1/4" BSP) | 3 |
| 5 mm Tube, 5 m length | 1 |
| Threaded rod (8 mm diam, 16 cm long) | 3 |
| Threaded rod (6 mm diam, 21 cm long) | 12 |
| Ball Bearing (NSK608) | 3 |
| Linear Rod (10 mm diam, 18 cm long) | 3 |
| Linear Bearing (LM10UU) | 6 |
| M8 Nut | 3 |
| M6 Nut and Washer | 48 |
| Power Supply (GPS-4303) | 1 |
| 100 $\mu$F Capacitor | 3 |

## References


[1] M. Spong, S. Hutchinson, and M. Vidyasagar, *Robot Modeling and Control*. Wiley, 2005.

[2] G. Robinson and J. Davies, "Continuum robots - a state of the art," in *Proceedings - IEEE International Conference on Robotics and Automation*, vol. 4, 1999, pp. 2849–2854.

[3] I. D. Walker, "Continuous backbone "continuum" robot manipulators," *ISRN robotics*, vol. 2013, 2013.

[4] D. Rus and M. Tolley, "Design, fabrication and control of soft robots," *Nature*, vol. 521, no. 7553, pp. 467–475, 2015.

[5] D. Trivedi, C. Rahn, W. Kier, and I. Walker, "Soft robotics: Biological inspiration, state of the art, and future research," *Applied Bionics and Biomechanics*, vol. 5, no. 3, pp. 99–117, 2008.

[6] L. Hines, K. Petersen, G. Lum, and M. Sitti, "Soft actuators for small-scale robotics," *Advanced Materials*, vol. 29, no. 13, 2017.

[7] J. Gul, M. Sajid, M. Rehman, G. Siddiqui, I. Shah, K.-H. Kim, J.-W. Lee, and K. Choi, "3d printing for soft robotics–a review," *Science and Technology of Advanced Materials*, vol. 19, no. 1, pp. 243–262, 2018.

[8] T. Wallin, J. Pikul, and R. Shepherd, "3d printing of soft robotic systems," *Nature Reviews Materials*, vol. 3, no. 6, pp. 84–100, 2018.

[9] B. Gorissen, D. Reynaerts, S. Konishi, K. Yoshida, J.-W. Kim, and M. De Volder, "Elastic inflatable actuators for soft robotic applications," *Advanced Materials*, vol. 29, no. 43, 2017.

[10] "Soft robotics toolkit," 2019, retrieved on 27/03/2019. [Online]. Available: https://softroboticstoolkit.com/components

[11] M. Cianchetti, C. Laschi, A. Menciassi, and P. Dario, "Biomedical applications of soft robotics," *Nature Reviews Materials*, vol. 3, no. 6, pp. 143–153, 2018.

[12] Y. Fu, H. Liu, W. Huang, S. Wang, and Z. Liang, "Steerable catheters in minimally invasive vascular surgery," *International Journal of Medical Robotics and Computer Assisted Surgery*, vol. 5, no. 4, pp. 381–391, 2009.

[13] X. Hu, A. Chen, Y. Luo, C. Zhang, and E. Zhang, "Steerable catheters for minimally invasive surgery: a review and future directions," *Computer Assisted Surgery*, vol. 23, no. 1, pp. 21–41, 2018.

[14] M. Calisti, G. Picardi, and C. Laschi, "Fundamentals of soft robot locomotion," *Journal of the Royal Society Interface*, vol. 14, no. 130, 2017.

[15] K. Quillin, "Kinematic scaling of locomotion by hydrostatic animals: Ontogeny of peristaltic crawling by the earthworm lumbricus terrestris," *Journal of Experimental Biology*, vol. 202, no. 6, pp. 661–674, 1999.

[16] S. Chatterjee, R. Niiyama, and Y. Kawahara, "Design and development of a soft robotic earthworm with hydrostatic skeleton," in *Proceedings - IEEE International Conference on Robotics and Biomimetics*, 2017, pp. 1–6.

[17] N. Saga and T. Nakamura, "Development of a peristaltic crawling robot using magnetic fluid on the basis of the locomotion mechanism of the earthworm," *Smart materials and structures*, vol. 13, no. 3, p. 566, 2004.

[18] B. Winstone, T. Pipe, C. Melhuish, M. Callaway, A. C. Etoundi, and S. Dogramadzi, "Single motor actuated peristaltic wave generator for a soft bodied worm robot," in *Proceedings - IEEE International Conference on Biomedical Robotics and Biomechatronics*, 2016, pp. 449–456.

[19] A. A. Calderón, J. C. Ugalde, J. C. Zagal, and N. O. Pérez-Arancibia, "Design, fabrication and control of a multi-material-multi-actuator soft robot inspired by burrowing worms," in *Proceedings - IEEE International Conference on Robotics and Biomimetics*, 2016, pp. 31–38.

[20] F. Connolly, P. Polygerinos, C. Walsh, and K. Bertoldi, "Mechanical programming of soft actuators by varying fiber angle," *Soft Robotics*, vol. 2, no. 1, pp. 26–32, 2015.

[21] C. Onal and D. Rus, "Autonomous undulatory serpentine locomotion utilizing body dynamics of a fluidic soft robot," *Bioinspiration and Biomimetics*, vol. 8, no. 2, 2013.

[22] M. Luo, M. Agheli, and C. Onal, "Theoretical modeling and experimental analysis of a pressure-operated soft robotic snake," *Soft Robotics*, vol. 1, no. 2, pp. 136–146, 2014.

[23] M. Luo, W. Tao, F. Chen, T. Khuu, S. Ozel, and C. Onal, "Design improvements and dynamic characterization on fluidic elastomer actuators for a soft robotic snake," in *Proceedings - IEEE Conference on Technologies for Practical Robot Applications*, 2014.

[24] T. Kalisky, Y. Wang, B. Shih, D. Drotman, S. Jadhav, E. Aronoff-Spencer, and M. Tolley, "Differential pressure control of 3d printed soft fluidic actuators," in *Proceedings - IEEE International Conference on Intelligent Robots and Systems*, 2017, pp. 6207–6213.

[25] B. Wijnen, E. Hunt, G. Anzalone, and J. Pearce, "Open-source syringe pump library," *PLoS ONE*, vol. 9, no. 9, 2014.

[26] K. Ikuta, H. Ichikawa, K. Suzuki, and D. Yajima, "Multi-degree of freedom hydraulic pressure driven safety active catheter," in *Proceedings - IEEE International Conference on Robotics and Automation*, 2006, pp. 4161–4166.

[27] K. Ikuta, Y. Matsuda, D. Yajima, and Y. Ota, "Pressure pulse drive: A control method for the precise bending of hydraulic active catheters," *IEEE/ASME Transactions on Mechatronics*, vol. 17, no. 5, pp. 876–883, 2012.

[28] J. Lake, K. Heyde, and W. Ruder, "Low-cost feedback-controlled syringe pressure pumps for microfluidics applications," *PLoS ONE*, vol. 12, no. 4, 2017.

[29] M. Appaji, G. S. Reddy, S. Arunkumar, and M. Venkatesan, "An 8051 microcontroller based syringe pump control system for surface micromachining," *Procedia Materials Science*, vol. 5, pp. 1791–1800, 2014.

[30] M. Cubberley and W. Hess, "An inexpensive programmable dual-syringe pump for the chemistry laboratory," *Journal of Chemical Education*, vol. 94, no. 1, pp. 72–74, 2017.

[31] D. Camarillo, K. Loewke, C. Carlson, and J. Salisbury, "Vision based 3-d shape sensing of flexible manipulators," in *Proceedings - IEEE International Conference on Robotics and Automation*, 2008, pp. 2940–2947.

[32] M. Dalvand, S. Nahavandi, and R. Howe, "High speed vision-based 3d reconstruction of continuum robots," in *Proceedings - IEEE International Conference on Systems, Man, and Cybernetics*, 2017, pp. 618–623.

[33] M. Hannan and I. Walker, "Real-time shape estimation for continuum robots using vision," *Robotica*, vol. 23, no. 5, pp. 645–651, 2005.

[34] K. Wu, L. Wu, and H. Ren, "An image based targeting method to guide a tentacle-like curvilinear concentric tube robot," in *Proceedings - IEEE International Conference on Robotics and Biomimetics*, 2014, pp. 386–391.

[35] M. Yip and D. Camarillo, "Model-less feedback control of continuum manipulators in constrained environments," *IEEE Transactions on Robotics*, vol. 30, no. 4, pp. 880–889, 2014.

[36] Y. Jin, Y. Wang, X. Chen, Z. Wang, X. Liu, H. Jiang, and X. Chen, "Model-less feedback control for soft manipulators," in *Proceedings - IEEE International Conference on Intelligent Robots and Systems*, vol. 2017-September, 2017, pp. 2916–2922.

[37] Y. Lu, C. Zhang, S. Song, and M. Q.-H. Meng, "Precise motion control of concentric-tube robot based on visual servoing," in *Proceedings - IEEE International Conference on Information and Automation*, 2017, pp. 299–304.

[38] M. S. Xavier, A. J. Fleming, and Y. K. Yong, "Experimental characterisation of hydraulic fiber-reinforced soft actuators for worm-like robots," in *Proceedings - International Conference on Control, Mechatronics and Automation (Accepted)*, 2019.

[39] S. Pandey and S. Sengupta, "Color detection and tracking from live stream—an extensive survey," *Int. J. Comput. Appl*, vol. 168, no. 3, 2017.

[40] H. H. A. Kadouf and Y. M. Mustafah, "Colour-based object detection and tracking for autonomous quadrotor uav," in *IOP Conference Series: Materials Science and Engineering*, vol. 53, no. 1. IOP Publishing, 2013, p. 012086.

[41] H. S. Parekh, D. G. Thakore, and U. K. Jaliya, "A survey on object detection and tracking methods," *International Journal of Innovative Research in Computer and Communication Engineering*, vol. 2, no. 2, pp. 2970–2979, 2014.

[42] X. Zhou, Y. Teng, and X. Li, "Development of a new pneumatic-driven earthworm-like soft robot," in *Proceedings - International Conference on Mechatronics and Machine Vision in Practice*, 2016, pp. 1–5.